Response properties in a model for granular matter

2000 J. Phys. A: Math. Gen. 33 4401

(http://iopscience.iop.org/0305-4470/33/24/301)

J. Phys. A: Math. Gen. **33** (2000) 4401–4426. Printed in the UK PII: S0305-4470(00)09511-1

Response properties in a model for granular matter

A Barrat† and V Loreto‡

† Laboratoire de Physique Théorique§, Bâtiment 210, Université de Paris-Sud, 91405 Orsay Cedex, France
‡ PMMH Ecole Supérieure de Physique et Chimie Industrielles, 10 rue Vauquelin, 75231 Paris Cedex 05, France

E-mail: `Alain.Barrat@th.u-psud.fr` and `loreto@pmmh.espci.fr`

Received 11 November 1999, in final form 6 April 2000

Abstract. We investigate the response properties of granular media within the framework of the so-called *random Tetris model*. We monitor, for different driving procedures, several quantities: the evolution of the density and of the density profiles, the ageing properties through the two-times correlation functions and the two-times mean-square distance between the potential energies, the response function defined in terms of the difference in the potential energies of two replicas driven in two slightly different ways. We focus, in particular, on the role played by the spatial inhomogeneities (structures) spontaneously emerging during the compaction process, the history of the sample and the driving procedure. It turns out that none of these ingredients can be neglected for the correct interpretation of the experimental or numerical data. We discuss the problem of the optimization of the compaction process and we comment on the validity of our results for the description of granular materials in a thermodynamic framework.

(Some figures in this article are in colour only in the electronic version; see `www.iop.org`)

1. Introduction

Granular media‖ are usually considered to be non-thermal systems because their thermal energy is so negligibly small with respect to other energy contributions (e.g. potential energy) that for all the practical purposes they are virtually at zero temperature. This feature draws a lot of consequences from the point of view of the validity of thermodynamics for such systems. One of the most important consequences is that, unless perturbed in some way (e.g. driving energy into the system), a granular system cannot explore its phase space spontaneously, but remains trapped in one of the numerous metastable configurations. One has then to look at the dynamics of a granular system always as a response to some perturbations and in general the response will depend in a non-trivial way on the rheological properties of the medium, on the boundaries, on the driving procedure and, last but not the least, on the past history of the system.

In this paper we focus on the response properties of a class of lattice models, the so-called random Tetris model (RTM) [2], that, despite their apparent simplicity are able to reproduce many features of real granular materials: slow-relaxations during compaction [2, 3], segregation [4], dilatancy properties [5] and ageing [6].

§ Unité Mixte de Recherche UMR 8627.
‖ For a recent introduction to the overall phenomenology see [1].

0305-4470/00/244401+26$30.00

We shall be concerned, in particular, with the interplay between the response properties and the spatial structures that emerge spontaneously as a consequence of the dynamics imposed on these systems. Several examples in this direction have already been drawn: the phenomenon of structures formation that plays a crucial role in explaining the complex features of internal avalanching [7] or the coarsening phenomena that parallel the vibration-induced compaction process (to be discussed in a forthcoming paper [8]).

We shall consider several procedures of vibro-compaction and we shall study how the system responds to different procedures and how the emerging inhomogeneities affect the response properties of these systems. The vibration procedures are specified in terms of the temporal function describing the evolution of the shaking amplitude. The simplest case is the one where one keeps the shaking amplitude constant indefinitely. More generally we shall consider complex procedures corresponding to sequences of cooling and annealing processes. In all the different cases we monitor several quantities. On the one hand, we focus our attention on global quantities such as the global density, the response and the correlation functions. On the other hand, we monitor some local quantities that allow us to investigate the large-scale structures emerging spontaneously in these systems as a response to the imposed perturbation (driving). The comparison between global and local quantities will be a valuable tool towards an understanding of how granular materials respond to perturbations and in this perspective of the importance of spatial structures.

Within this framework we can address several questions. One of the first issues we can investigate is the importance of the history, i.e. the specific procedure undergone by the sample before we perform our measurements. It is interesting to ask where the history of the system is encoded and, for instance, whether the global density represents a good parameter for the description of a static packing or one needs to specify other parameters. The analysis of the correlation functions will allow us to investigate under which conditions the systems exhibit ageing behaviour. On the other hand, with the knowledge of the effect of different kinds of perturbation, we shall address the problem of the optimization of the compaction procedures that can be stated as follows: single out the best sequence of perturbations to impose onto the system in order to maximize the density measured in a suitable part of the system.

Our results will also allow us to comment on the existence of transitions in the response properties and on recently published results concerning the violation of the fluctuation–dissipation theorem (FDT) for granular media [9].

This paper is organized as follows. In section 2 we recall the model definition, we define the different dynamical procedures and we introduce the quantities we shall look at for the analysis of the response properties. Sections 3 and 4 are devoted to the analysis of the response properties during a process of continuous shaking at constant amplitude and during cyclic procedures, respectively. In section 5 we discuss globally all the results comparing different procedures and different histories and commenting on the consequences from the thermodynamic point of view. Finally, in section 6 we draw our conclusions.

2. Model definition

The essential ingredient of the RTM [2] is the geometrical frustration that for instance in granular packings is due to excluded-volume effects arising from the differently shaped particles. This geometrical feature is captured in this class of lattice models where all the basic properties are brought by the particles and no assumptions are made about the environment (lattice). The interactions are not spatially quenched but are determined in a self-consistent way by the local arrangements of particles. Despite the simplicity of their definition, these systems present a highly complex phase space and their dynamics generates automatically

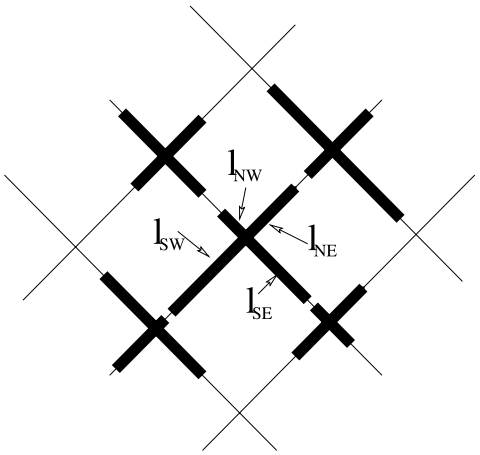

Figure 1. Sketch of a local arrangement of particles in the random Tetris model: each particle can be schematized in general as a cross with four arms of different lengths, denoted by $l_{NE}, l_{NW}, l_{SE}, l_{SW}$, chosen in a random way.

a very rich gallery of time–space correlations: time-scales, spatial structures, memory, etc. Furthermore, they show a very interesting interplay between the dynamics and the time–space structures. It is worth noting how in this class of models the origins of randomness and of frustration coincide because both are given in terms of the particle properties.

Let us recall briefly the definition of the model, which includes, like in the real computer game *Tetris*, a rich variety of shapes and sizes. On a lattice each particle can be schematized in general as a cross with four arms (in general, the number of arms is equals to the coordination number of the lattice) of different lengths, denoted by $l_{NE}, l_{NW}, l_{SE}, l_{SW}$, chosen in a random way. An example of particle configuration on a tilted square lattice is shown in figure 1.

The static properties of the system are then completely characterized by giving the random numbers defining the particles. These numbers are given once for all particles and it is clear how in this way one has a complete freedom in the choice of the system; the models used in [3, 4] are particular cases of the general model where one has chosen the particle sizes and shapes in a deterministic way.

The interactions among the particles obey the general rule that one cannot have superpositions. For instance, one has to check that for two nearest-neighbour particles the sum of the arms oriented along the bond connecting the two particles is smaller than the bond length. It turns out that in this way the interactions between the particles are not fixed once and for all but they depend on the complexity of the spatial configuration. We shall return to this point later on in connection with the interplay between the dynamics and the emergence of spatial structures.

The extreme generality of the model definition allows a large variety of choices for the particles. Just to give an idea of how the system can be chosen, let us consider two different versions of the RTM that we shall denote by A and B.

(A) A system with random elongated particles. This case represents the direct generalization of the system considered in [3]. Instead of considering two types of elongated particles with fixed sizes we consider elongated particles whose size is chosen randomly according to the expressions $l_{NE} = l_{SW}, l_{NW} = l_{SE}, l_{NE} = \frac{3}{4}d \pm 0.1d\eta, l_{NW} = d - l_{NE}$ and equivalently for the other orientation. η represents a random variable distributed uniformly in [0, 1].

(B) A system with random particles with spherical symmetry. In this case we have particles whose size is chosen randomly according to the expressions $l_{NE} = l_{SW}$, $l_{NW} = l_{SE}$, $l_{NE} = \frac{1}{2}d \pm 0.2d\eta, l_{NW} = \frac{1}{2}d \pm 0.2d\eta$.

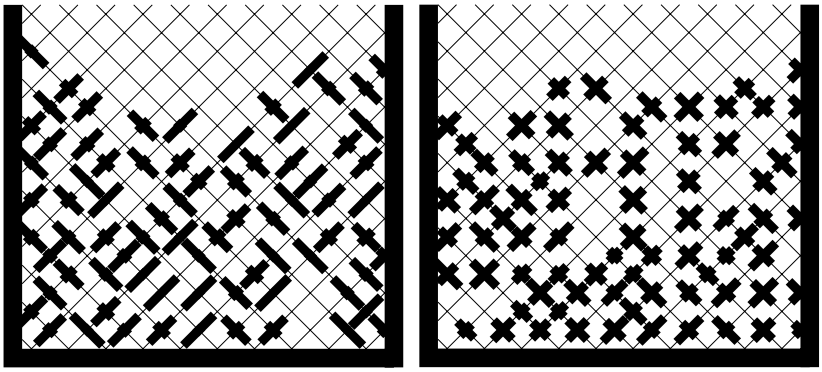

Figure 2. Example of a stable packing configuration for a system of type A (left) and B (right) (see text). In all our simulations we used particles of type A.

In all our simulations we have always used, without loss of generality, systems with particles of type A. With the above given rules one can define the allowed configurations. For instance by introducing gravity one can decide whether a certain configuration (packing) is mechanically stable or not. For instance, figure 2 shows examples of mechanically stable configurations under gravity for the cases A and B. In these cases a tilted square lattice was used to implement the existence of a preferential direction in the system.

The dynamics will then consist in general of a diffusion constrained by the particle geometry. In the following sections we shall be concerned with the case of the vibration-induced compaction phenomenon [10].

One of the possible ways to implement a vibration or a shaking procedure in the RTM model is to consider a Monte Carlo dynamics where the particles diffuse on the lattice according to some rules, as explained below. One can actually choose the specific dynamics in several ways. In the following we discuss some examples.

The system is initialized by filling the container idealized as a lattice with lateral periodic boundary conditions and a closed boundary at the bottom. The procedure of filling consists in inserting the grains at the top of the system, one at a time, and letting them fall down, performing, under the effect of gravity, an oriented random walk on the lattice, until they reach a stable position, say a position in which they cannot fall further. This filling procedure is realized by the addition of one particle at a time and stops when particles can no longer enter the box from the top.

In the case of shaking the dynamics can be divided into several alternating steps where the system is perturbed by allowing the grains to move in any allowed directions with a probability p_{up} to move upwards (with $0 < p_{up} < 1.0$) and a probability $p_{down} = 1 - p_{up}$ to move downwards. Each step lasts until a fixed number of N moves per particle have been attempted with a fixed value of $x = p_{up}/p_{down}$. The quantity x can be related to the adimensional acceleration Γ used in compaction experiments [10] through the relation $\Gamma \simeq 1/\log(1/\sqrt{x})$.

More precisely the single dynamical step consists of the following operations:

(a) extracting a grain with uniform probability;
(b) extracting a possible movement for this grain among the nearest neighbours according to the probabilities p_{up} and p_{down};
(c) moving the grain if *all* the possible geometrical constraints with the neighbours are satisfied.

One is then free to choose the desired sequence of steps depending on the quantities one wants to monitor or on the experimental procedures one wants to reproduce.

The easiest possibility is the *continuous shaking* realized by letting the system evolve continuously with a fixed and constant x. We shall discuss this case in section 3. Another possible procedure, explored in [3], mimics the process of tapping and it comprises two alternating steps. First, in a 'heating' process (tapping) the system is perturbed by allowing the grains to move in any allowed directions with a probability p_{up} to move upwards and a probability $p_{down} = 1 - p_{up}$ to move downwards. After each tapping has been completed (i.e. a fixed number of N moves per particle have been attempted with a fixed value of $x = p_{up}/p_{down}$) we allow the system to relax setting $p_{up} = 0$. The relaxation process ('cooling') is supposed to be completed when particles can no longer move under the effect of gravity, i.e. unless p_{up} is switched on. After this relaxation the system is in a stable static state and one restarts the cycle.

More generally one can define complex cycles where one changes the value of x during the evolution of the system according to some specific temporal function. This is the most general case that allows one to impose specific histories. We shall discuss this case in section 4.

Before describing the results in a detailed way, let us define the different quantities we shall be monitoring during the shaking procedure. Denoting with (i, j) the coordinates of a generic site, where i indicates the horizontal coordinate and j the vertical one along the direction of gravity, we can define with $m(i, j)$ the mass content of the site (i, j) in such a way that $m(i, j) = 1$ if the site contains a particle and $m(i, j) = 0$ otherwise. With these definitions in mind we shall monitor the evolution of the following quantities.

Density profile. The density profile gives the value of the density (averaged over horizontal layers) as a function of the height. It represents the simplest, though rough, way to characterize the inhomogeneities in the system: since the gravity is acting in the vertical direction, we concentrate on the heterogeneities that can occur in this direction. In formulae we have

$$p(j, t) = \frac{1}{L} \sum_{i=1}^{L} m_{i,j}(t) \qquad \text{for} \quad j \in [0 : M] \tag{1}$$

where L is the width of the system and M is its maximal height.

Average density. The density of the packing, i.e. the fraction of sites occupied with respect to the total number of sites, is measured after each relaxation step and, in correspondence with real experiments, we plot the behaviour of this density as a function of time. In order to avoid finite-size effects we considered systems with a linear size of at least $L = 50$ sites and, in order to be sure of observing bulk effects, we measured the density in the lower 25% or 50% of the system.

Response function. The response function is defined as the change in the potential energy of the system for a small change in the value of x. What we do in practice is evolve the system for a certain time t_w. At t_w we define a replica of the system whose mass content will be described by $m^r_{i,j}$ and we let the original system evolve with the same x and the replica with $x' = x + \delta x$, where δx is small enough to keep the linear response approximation valid. At times larger than t_w we monitor the evolution of the potential energy for the two replicas defined as $P(t + t_w) = \sum_{i,j} m_{i,j}(t + t_w)(j + 1)$ and $P_r(t + t_w) = \sum_{i,j} m^r_{i,j}(t + t_w)(j + 1)$. The

response of the system is defined as

$$R(t+t_w, t_w) = \frac{P_r(t+t_w) - P(t+t_w)}{N_{part}} \tag{2}$$

where N_{part} is the total number of particles in the system. We also monitor the density profile of the replica, $p^r(j, t+t_w)$, and the difference $\Delta p(j, t+t_w) = p^r(j, t+t_w) - p(j, t+t_w)$ between the profiles. Note that $R(t+t_w, t_w)$ can also be written as $R(t+t_w, t_w) = \sum_j \Delta p(j, t+t_w)(j+1)L/N_{part}$.

Correlation functions. We have considered two kinds of measures of the temporal correlations. The two-times mass–mass correlation function, defined as

$$C(t+t_w, t_w) = \frac{1}{N_{part}} \overline{\sum_{i,j} (m_{i,j}(t+t_w)\, m_{i,j}(t_w))} \tag{3}$$

and the mean-square distance between the potential energies at times t_w and $t+t_w$, defined as

$$\begin{aligned} B(t+t_w, t_w) &= \overline{\left(\frac{\sum_{i,j}(j+1)\, m_{i,j}(t+t_w)}{N_{part}} - \frac{\sum_{i,j}(j+1)\, m_{i,j}(t_w)}{N_{part}} \right)^2} \\ &= \overline{\left(\overline{h}(t+t_w) - \overline{h}(t_w)\right)^2} \end{aligned} \tag{4}$$

where the overbar indicates the average over different realizations and $\overline{h}(t)$ indicates the height of the centre of mass at time t.

It is worth noting that we decided to measure the two-times mass–mass correlation function via equation (3) instead of the two-times correlation function for the global density [6] because, as will become clear in the following, the definition of the global density is somehow arbitrary in these systems with a preferential direction imposed by gravity.

We have used system sizes $L \times M$ of 60×60, 120×60 and 60×120 to ensure that finite-size effects were irrelevant. We let the system evolve for 10^6 Monte Carlo steps per particle after a preparation (waiting at constant x or other more complicated histories) during up to 10^6 Monte Carlo steps per particle. Averaging was performed on up to 1000 samples.

3. Response properties of a system subject to continuous shaking

In this section we present the results of the simulations for a system subject to continuous shaking at constant x.

The mean density, calculated in the lower 25% and 50% of the box, grows slowly, from an initial value ρ_0. This value is not universal but depends on the choice of particles and on the fraction of the system where one performs the average. Figure 3 shows the evolution of the density measured in the lower 25% and 50% of the system for different values of x. It is interesting to note that there exists an optimal value of x that allows one to obtain the maximal density in the fraction of the system considered for the averaging procedure. At small times this optimal value depends on time due to the crossing of the different curves. This fact already suggests that, in order to compactify the system, the optimal strategy will not be to keep x constant, but rather to vary it. This type of behaviour was also observed recently in the parking-lot model [11]. However, in our case the mechanism responsible for these phenomena can be understood by looking at the density profiles (see below), a concept which is absent in the parking-lot model. Moreover, if we compare the data for the bulk density computed as

25% or 50% of the bulk, we see that the curves differ and that the optimal value of x is around $x \simeq 0.6$ in the first case, and around $x \simeq 0.8$ in the other. This feature can be explained by noticing the combined effect of two factors: on the one hand, the bulk compactifies better for larger x. For example, in the data of [10], taken at the bottom of the sample, the density is an increasing function of the shaking amplitude; on the other hand, increasing x, the interface becomes broader and can affect the global bulk density effectively reducing it. As a result there will be an optimal x which for instance is smaller considering the measure of the density in the lower 50% of the system with respect to the measure in the lower 25% because one needs a larger x in order to extend the interface deeper and deeper. This phenomenology represents an indication that heterogeneities are quite relevant and that particular attention needs to be taken in defining the observed quantities. Our finding of an optimal shaking amplitude is, in fact, in agreement with previous experimental results [10]. We recall for this that x and the adimensional acceleration Γ can be linked by the relation $\Gamma \simeq 1/\log(1/\sqrt{x})$. In compaction experiments [10] it was observed that the density, measured on the lowest part of the system, was an increasing function of the shaking amplitude. However, the authors were expecting this density to 'decrease upon further acceleration increase', since their experiments probed only the regime of relatively low shaking intensity. Moreover, such a decrease is expected to be more apparent in two-dimensional systems [12], which is the case of our model.

The growth law for the density has been shown by various authors to be, experimentally [10] and for many models [3, 13], well described by the functional form

$$\rho(t) = \rho_\infty - \frac{\rho_\infty - \rho_0}{1 + B\ln(1 + t/\tau)} \tag{5}$$

where ρ_∞, the asymptotic density, B and τ are fitting parameters depending on the shaking amplitude. Also in our case equation (5) is satisfied and one can actually collapse all the curves into a unique logarithmic function. Figure 4 shows the collapse of the density curves measured in the lower 50% of the system (one obtains similar results using the curves of the density measured in the lower 25% of the system) for three different values of x ($x = 0.1,\ 0.6,\ 0.7$) and for different values of t_w (i.e. the measure of the density begins at t_w instead of 0, which of course changes the parameters in equation (5)): the functional form is tested by plotting the rescaled density $(\rho(t) - \rho_0)/(B(\rho_\infty - \rho(t)))$ versus $\tilde{t} = t/\tau$, and comparing it with $\ln(1 + \tilde{t})$.

In all cases the functional form (5) is quite well satisfied with τ simply proportional to t_w, ρ_∞ being a bell-shaped function of x† and B exhibiting a complex dependence on t_w and x. Several remarks are in order. The fitting parameters depend on the fraction of the system where one measures the density. On the other hand, the logarithmic fit starts to be valid after a transient time of the order of 50–500 iterations depending on x and on the fraction of the system used for the measurements. This behaviour is quite understandable. Before compaction can start in the bulk a weak decompaction is in order which is stronger for higher x and which extends at longer times if one is measuring the density in a deeper region. One can actually notice the decompaction process in figure 3, especially for large values of x. Only after the decompaction process ends can one hope for equation (5) to be valid. This is the reason why we have considered the collapse of the density curves obtained after a suitable waiting time t_w.

A different way of measuring the compaction is to look at the mean height, or potential energy P defined in section 2. In this case, the whole system is considered. We see in figure 5 that, also in this case, there exists an optimal value of x for which one has the lowest position of the centre of mass. Also in this case we find an agreement with the experimental findings

† ρ_∞ depends on x and is not 1 as in the simplest Tetris model [3], where the existence of a ground state with a perfect antiferromagnetic ordering allows the configuration at a density of 1. In the RTM the random choice of particles removes this limitation.

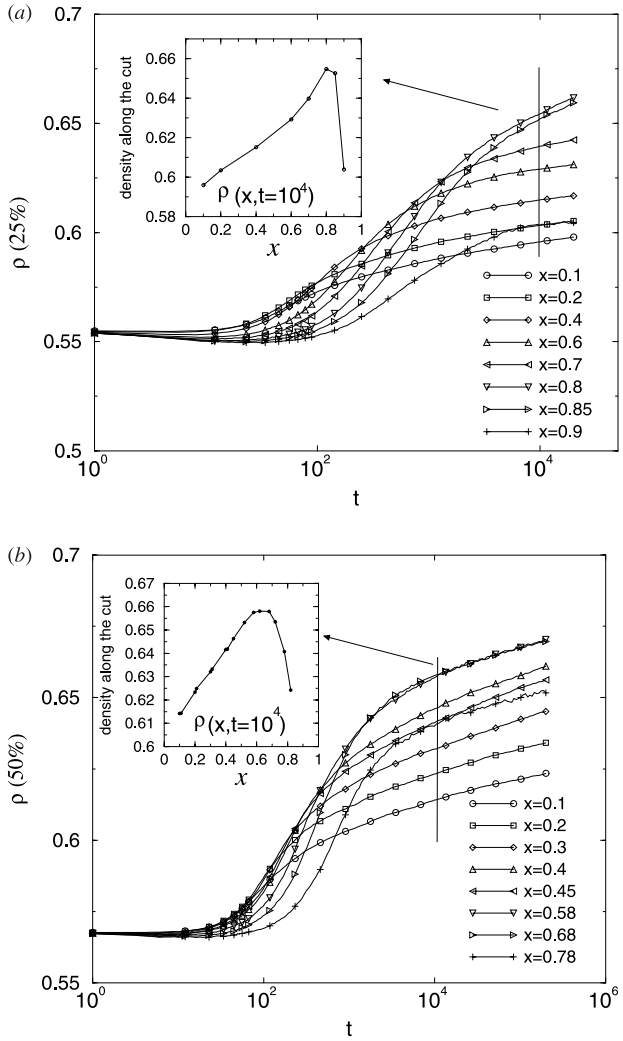

Figure 3. Time-evolution of the bulk density ((*a*) 25% and (*b*) 50% of the system) for several shaking amplitudes. The insets show the density at time $t = 10^4$ as a function of x. Note in both cases the existence of an optimal value of x, that depends on the fraction of the system where one measures the average density.

of [10] where the density measured from the height of the system was an increasing function of the shaking amplitude, while the authors expected the presence of a peak 'upon further acceleration increase'.

It is, however, already clear how the previous measurements, which are averages over the whole (or over an extensive part) of the system, cannot represent comprehensive information about the system. For example, in the measure of the mean height the interface gives a large contribution, while it is practically negligible if one is interested in bulk properties. Therefore, before turning our attention to a more detailed description of the system let us now study the two-times correlation function $C(t + t_w, t_w)$ which, as usual in ageing phenomena [14], gives a determination of the age of the system, since it depends on t and on t_w.

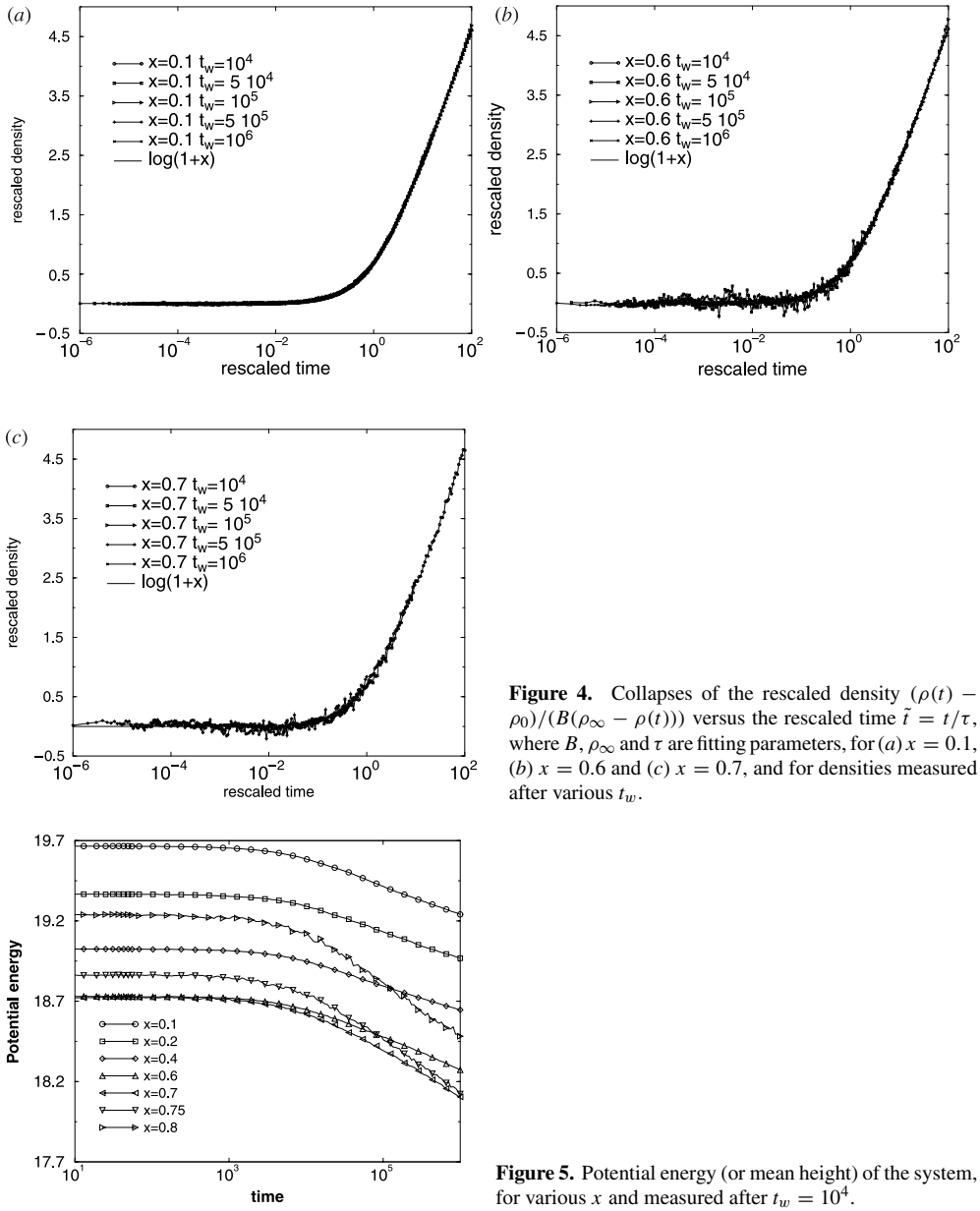

Figure 4. Collapses of the rescaled density $(\rho(t) - \rho_0)/(B(\rho_\infty - \rho(t)))$ versus the rescaled time $\tilde{t} = t/\tau$, where B, ρ_∞ and τ are fitting parameters, for (a) $x = 0.1$, (b) $x = 0.6$ and (c) $x = 0.7$, and for densities measured after various t_w.

Figure 5. Potential energy (or mean height) of the system, for various x and measured after $t_w = 10^4$.

In figures 6 and 7 we show the behaviour of $C(t + t_w, t_w)$ for several values of x and t_w. We observe for this model the typical ageing behaviour, with a first part for $t \ll t_w$ approaching a quasi-equilibrium curve where time-translation invariance is respected (i.e. for $t \ll t_w$, $C(t + t_w, t_w)$ approaches a curve depending only on t) a plateau, and, at $t \gg t_w$, a second decay, dependent on t_w, corresponding to ageing. We note that this behaviour, which is very common in ageing phenomena [14], is more realistic than that of the simplest Tetris model [3], where the plateau is at $C = 1$, so that only the second decay is observed [6]. As t_w grows, the plateau is better defined and the second decay appears at longer times.

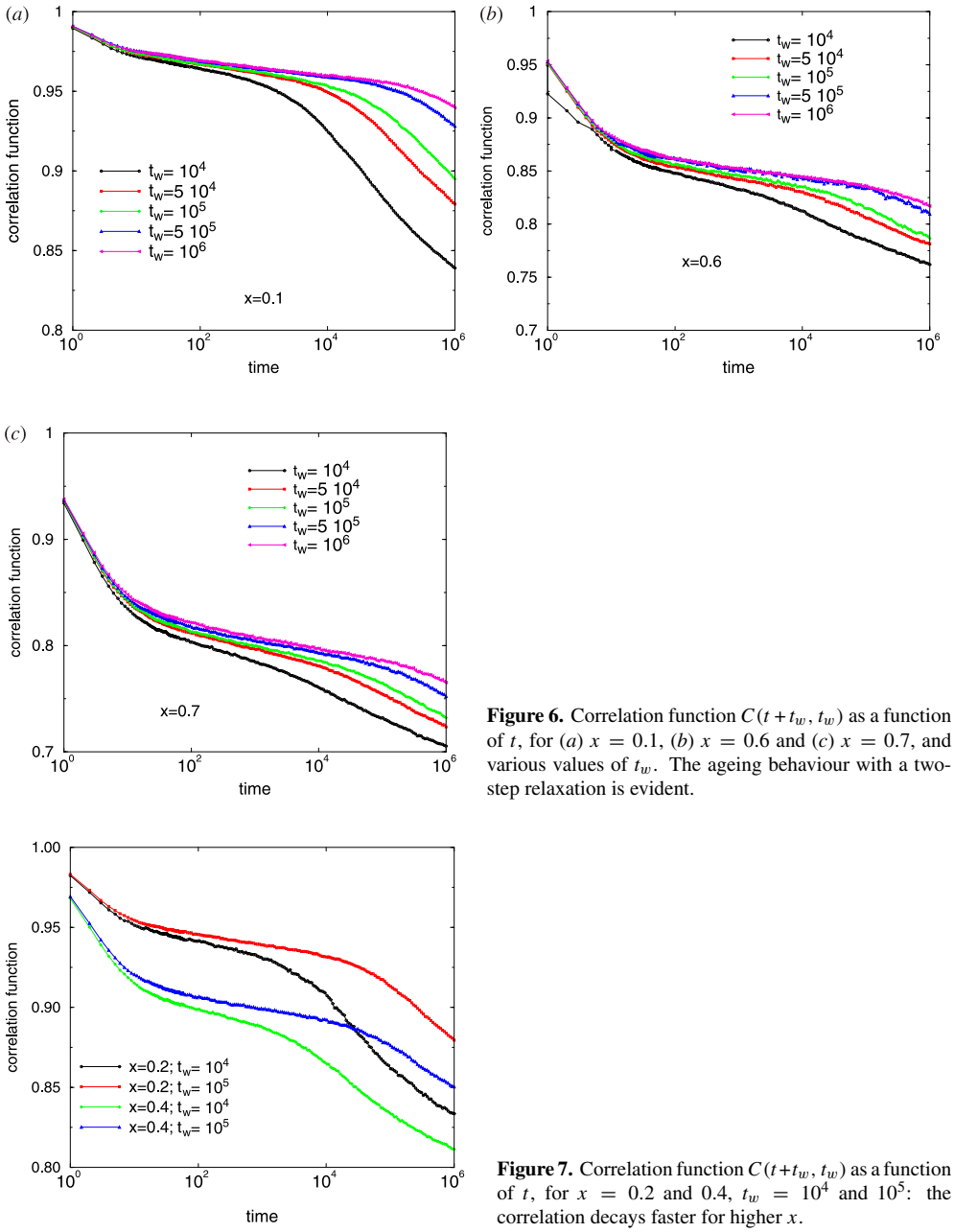

Figure 6. Correlation function $C(t+t_w, t_w)$ as a function of t, for (*a*) $x = 0.1$, (*b*) $x = 0.6$ and (*c*) $x = 0.7$, and various values of t_w. The ageing behaviour with a two-step relaxation is evident.

Figure 7. Correlation function $C(t+t_w, t_w)$ as a function of t, for $x = 0.2$ and 0.4, $t_w = 10^4$ and 10^5: the correlation decays faster for higher x.

The global properties of the correlation function depend smoothly on the shaking amplitude: as x grows, the correlation decays faster, as shown in figure 7. However, the curves do not differ qualitatively and have similar shapes.

In [6] the two-times correlation function for the global density was measured in the simplest version of the Tetris model. In this case it was proposed that the relaxation was of the form $\ln(t)/\ln(t_w)$ (the exact proposed form was $(1 - c_\infty)\ln((t_w + t_s)/\tau)/\ln((t + t_w + t_s)/\tau) + c_\infty$, where c_∞, t_s and τ were three fitting parameters), for very small values of x (in the range

$[10^{-4}; 10^{-1}]$). This form could fit all the curves since, as already mentioned, the first decay was non-existent.

Since, as has been pointed out in the above discussion, the definition of the system density is somehow arbitrary, we decided to measure the two-times mass–mass correlation function via equation (3). In our case, we only attempt to fit the second decay, i.e. the ageing part; since we expect weak ergodicity breaking [15], we propose a form going to zero at long times:

$$C(t + t_w, t_w) = \frac{a}{1 + b \ln(1 + t/\tau)} \qquad \text{for} \quad t \gg t_w \tag{6}$$

with a, b, τ fitting parameters. We show in figures 8 and 9 that we can collapse the curves using equation (6) and plot the rescaled correlation function $\tilde{C}$ versus the rescaled time $\tilde{t}$ according to

$$\begin{aligned} \tilde{C} &= \frac{bC}{a + (Ab - 1)C} \\ \tilde{t} &= t/\tau \end{aligned} \tag{7}$$

and obtain $\tilde{C} = 1/(A + \ln(1 + \tilde{t}))$. A is an irrelevant parameter introduced to avoid the divergence of $\tilde{C}$ at $\tilde{t} \to 0$, and whose value can be read in the figures. The behaviour of the fitting parameters is the following: a is roughly constant, while τ evolves proportionally to t_w, and b as the inverse of the logarithm of t_w. This leads to the conclusion that the overall behaviour of $C(t + t_w, t_w)$ is of the form $\log(t_w + t)/\log(t_w)$. We note that this is in agreement with the findings of [6], on a much wider range for x, but in contrast with the parking-lot model, for which a t/t_w behaviour has been observed [16], where, as in [6], a different definition of the correlation function was used: the correlation function of the densities. An experimental measure of the correlation functions would be welcome to discriminate between these predictions.

For completeness, we show in figure 10 the behaviour of the mean-square distance between the potential energies, $B(t+t_w, t_w)$ defined in the introduction though equation (6). $B(t+t_w, t_w)$ is an increasing function of t, displaying ageing behaviour with two steps separated by a plateau, as for the correlation function.

Before turning our attention to the response function defined in equation (2) let us add one important piece of information concerning the density profiles. It turns out, in fact, that it is essential to look at the inhomogeneities in the system in order to correctly interpret the response results. We shall do this by looking at the density profiles and at the differences between the profiles of the system and its perturbed replica, which will give information on the spatial structures, at least along the vertical direction.

We have monitored the density profiles $p(j, t)$, as defined in equation (1), of the system and of its replica after t_w. While the curves of the evolution of the bulk density (or of other global quantities like C or B) have similar shapes for all values of x (equation (5) and figure 3), the density profiles can exhibit very different behaviours. In figure 11, we display the short-time ($t = 0$–10^4) evolution of the profile for several values of the shaking amplitude, starting from the same profile for all values of x. In figure 12, we display the successive evolution, for $t_w < t < t_w + 10^6$ with $t_w = 10^4$. The first observation is that the width of the interface is larger for higher shaking amplitudes, which is a quite intuitive result. Moreover, we see that, for small shaking amplitudes, a very dense layer forms just under the interface. This layer (whose height is of five to ten lattice sites) is able to block the compaction process: in order to make the system more compact particles have to also rearrange in the bulk, and the dense layer acts as a barrier. The bottom part of the sample is therefore almost not evolving, as shown in figure 12. As time evolves the dense layer becomes broader, though in a very slow way. In all

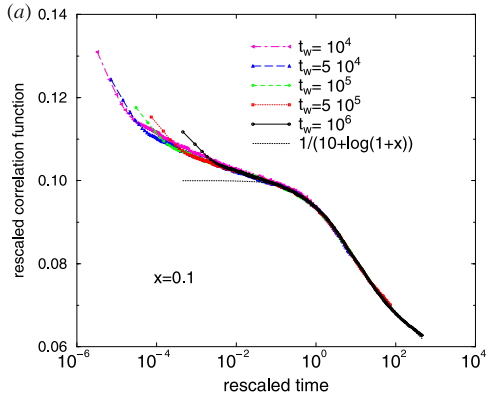

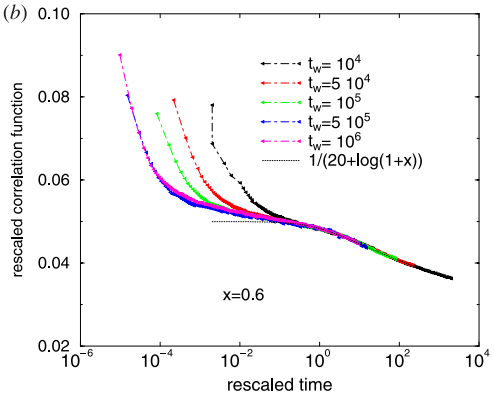

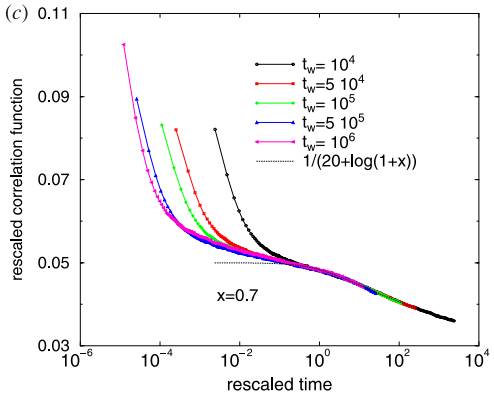

Figure 8. Collapse of the ageing part of the curves for the same values of x and t_w (five values for each x) as in figure 6; the rescaled correlation (see text) is plotted versus the rescaled time t/τ, and compared with the form $1/(A+\ln(1+\tilde{t}))$; the first part of the curves, not collapsed, corresponds to the first relaxation (approach to a quasi-equilibrium behaviour).

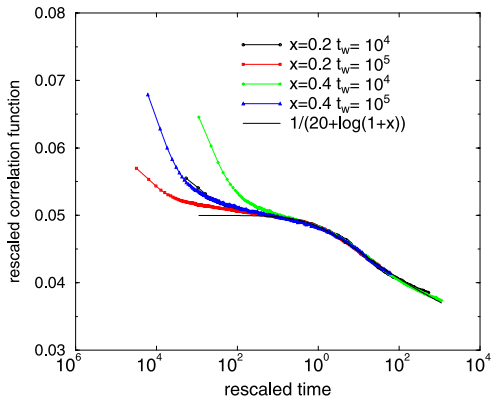

Figure 9. As in figure 8 for $x = 0.2$ and 0.4.

cases, the comparison of figures 11 and 12 also shows that the short-time dynamics is much faster than the successive evolution.

We note that these results are in agreement with experimental results showing that, at not too large shaking amplitude, the compaction is more efficient in the higher parts of the media (see the first reference in [10]) and that the locally measured density is larger in higher parts of the sample.

For higher x, diffusion is easier, and the layer forming at the top is less dense, broader and evolves faster (see in figure 12 the evolution of the dense layer for $x = 0.1,\ 0.2,\ 0.4,\ 0.6$); the

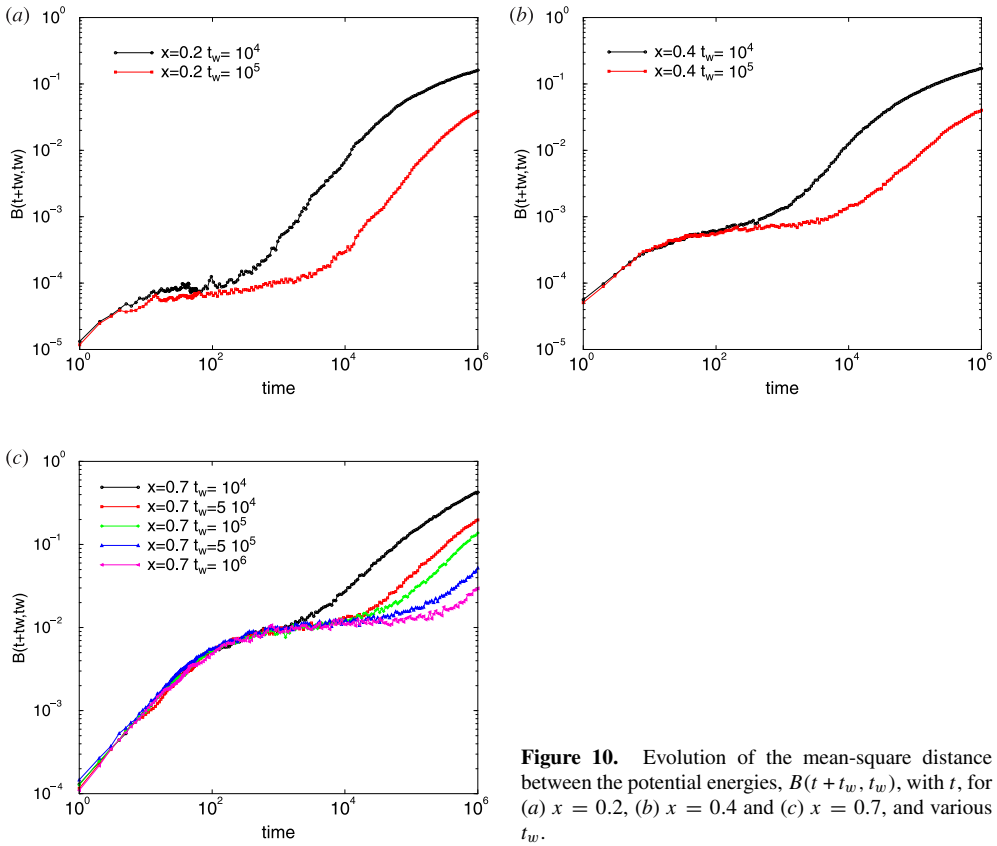

Figure 10. Evolution of the mean-square distance between the potential energies, $B(t+t_w, t_w)$, with t, for (*a*) $x = 0.2$, (*b*) $x = 0.4$ and (*c*) $x = 0.7$, and various t_w.

compaction process in the bulk is therefore facilitated: thus, even if the interface is broader, which could indicate a less dense system, the bulk will be able to compactify much better. The global density can therefore, in fact, be enhanced. This explains that, at least at finite times, the curves of the density can be higher for higher x, while one would expect the contrary starting from a dense system; of course, for very strong shaking, the system is very loose and the interface is very wide: this explains the existence of an optimal shaking amplitude for compaction (see figure 3) and, as mentioned before, why this optimal amplitude depends on the method of defining the bulk (it corresponds roughly to the value of x for which the interface attains the defined bulk).

We again have an indication of the importance of looking at the density profile: two very different profiles can have the same bulk density or potential energy (mean height).

Let us now turn to the analysis of the response function. As described in the introduction, we let the system evolve at constant x during a certain waiting time t_w, and then make a copy of the system, which we submit to a slightly different shaking, i.e. $x + \mathrm{d}x$. We have mostly used $\mathrm{d}x = 0.01$, and checked with $\mathrm{d}x = 0.005$ and $\mathrm{d}x = 0.02$ that the system was in the linear response regime (especially for $x = 0.1$ for which $\mathrm{d}x = 0.01$ is 10% of x).

The response function has been introduced in section 2 through equation (5): it is defined as the difference between the potential energy of the two copies of the system. Therefore, a *positive* response means that the perturbed system (at higher x) has a higher energy, and therefore it is *less compact* than the unperturbed one. This is what one clearly expects at high x for example, where the system is very loose and a higher x means that the particles are less

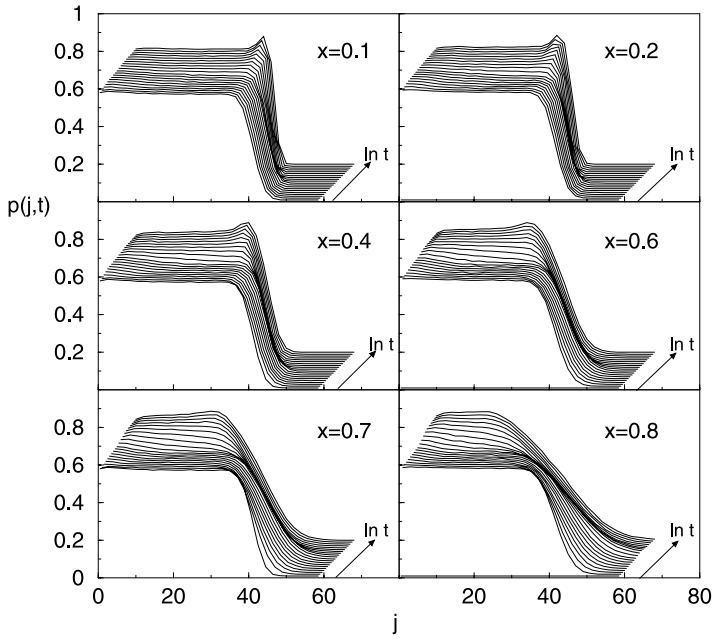

Figure 11. Density profiles for various values of x, evolving in time ($t = 0$–10^4), with no waiting time: the evolution starts from the same profile for all values of x. We see the formation of a dense layer for small x, and the evolution towards a smoother profile for large x.

subject to gravity. On the other hand, a *negative* response means that the perturbed system is *more compact* than the unperturbed one. This is not to be excluded *a priori*, since we have already seen in figure 3 that the density at a fixed time is not a monotonic function of x.

For $x = 0.1$, we indeed see (figure 13) that the response exhibits first a positive branch followed, after a certain time that depends on x and t_w, by a negative branch. The system is first relatively decompactified by the perturbation (positive response), but then, at later times, it compactifies better. This phenomenon was first noted in the case of the Tetris model in [9], where, however, only small values of t_w were used, and more emphasis was given to the negative part. For a fixed x, however, as t_w grows, the positive part extends to longer times and cannot be neglected.

As x grows, the positive part gets a higher amplitude and extends to longer times, and for $x \geqslant 0.7$ no negative response can be reached (figures 13 and 14).

This apparently odd behaviour can be understood by looking at the density profiles, and especially at the differences of the profiles between the perturbed and unperturbed systems, i.e. at the spatial distribution of the response. The response consists of two main contributions. On the one hand, the interface gives a positive response, i.e. a larger x will naturally lead to a looser interface, because a larger x means a higher probability for the particle to move upwards. On the other hand, however, the effect on the bulk is less obvious, since the particles can be blocked by those situated above (as is the case at small x, with the dense layer appearing), and need a global rearrangement of other particles in order to be able to move.

We show in figure 15 how the difference $\Delta p(j, t + t_w) = p^r(j, t + t_w) - p(j, t + t_w)$ as a function of j evolves in time after t_w. A positive $\Delta p(j, t + t_w)$ means that the perturbation has locally (at height j) compactified better (giving a local positive contribution to the response function), while a negative $\Delta p(j, t+t_w)$ corresponds to a locally less compact perturbed system

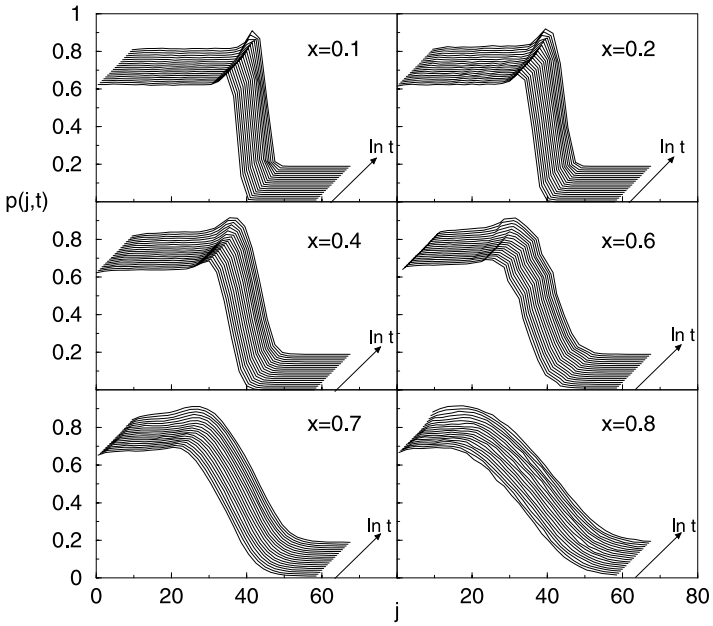

Figure 12. Density profiles for various values of x, evolving in time ($t = 0$–10^6) after a waiting time $t_w = 10^4$. The interface is broader for higher x, and the dense layer below the interface is more pronounced and evolving more slowly for lower x. Comparing with figure 11, we see that the overall evolution is much slower in all cases.

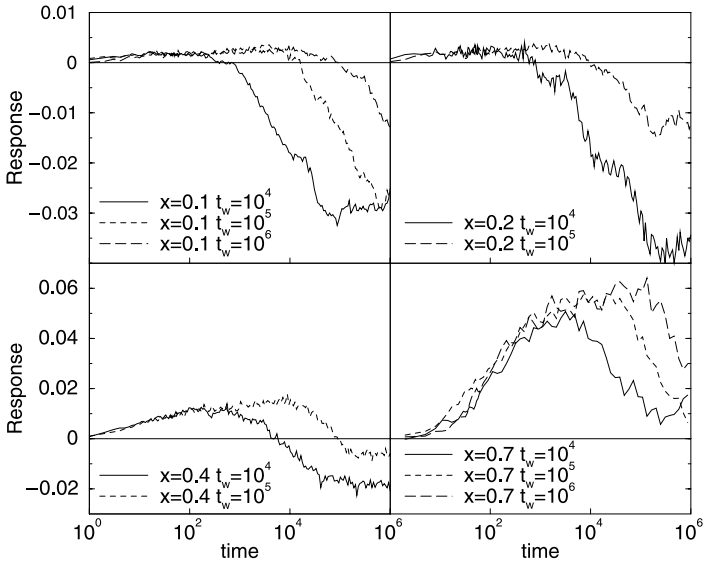

Figure 13. Response function $R(t + t_w, t_w)$ versus t, for several values of x and t_w. The vertical scale is the same for the left- and right-hand parts. The response tends to remains positive for a longer time when either x or t_w are higher.

(local negative contribution to the response function). Besides, recalling the definition of the response function, $R(t + t_w, t_w) = \sum_j \Delta p(j, t + t_w)(j + 1)L/N_{part}$, it is important to remark

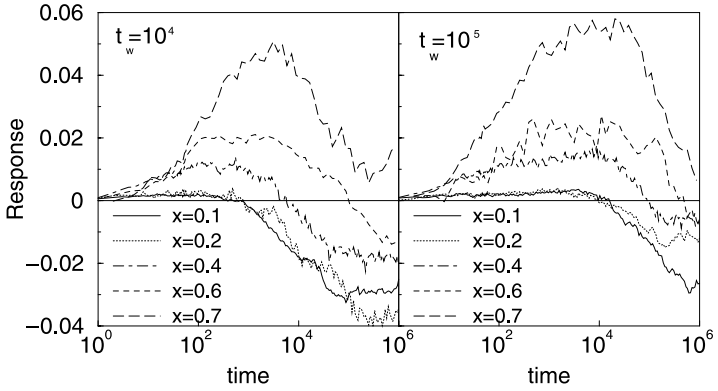

Figure 14. Response function $R(t + t_w, t_w)$ versus t, for $t_w = 10^4$ (left) and $t_w = 10^5$ (right), showing that, at fixed t_w, the response is an increasing function of x.

that the values of $\Delta p(j, t + t_w)$ coming from the interface (large j) bring a strong contribution to the response due to the term $(j + 1)$.

At low x ($x = 0.1$), the bulk is blocked by the thick dense layer just below the interface, as shown in figure 12. Therefore, the first effect of the perturbation dx is just to decompactify the interface, which gives rise to a positive R. However, once the interface is loosened, particles in the bulk may be allowed to rearrange more freely, and we obtain therefore a better compaction of the bulk, and a negative R. This phenomenon is shown in figure 15 by the creation of a dip at heights j just below the interface, with a bump $p^r(j, t) > p(j, t)$ just above the interface at low t, and then by the decrease of this bump with a mass transfer toward the low-j values of the dip. Let us remark, however, that a negative response, which means a better compaction for the perturbed replica, does not give any substantial change in the profile: the response to the perturbation is very heterogeneous, and the bottom part of the sample simply does not feel it. As t_w grows, the interface and the dense layer become more and more compact, and therefore harder and harder to decompactify. This explains why the response function stays positive for longer times: the decompaction process takes longer and longer (figure 16).

At higher values of x, the interface becomes smoother, the blocking layer becomes less dense and the effect of the perturbation on the interface becomes stronger and stronger. At strong shaking, i.e. large values of x, only the interface contributes to the response function, which therefore is positive at all times. We see in figure 15 that the effect of the perturbation is to transfer particles upwards.

In summary, as either t_w or x grows, the bulk is more compact, and therefore its contribution to the response is smaller. The response function tends to become positive due to the contribution of the interface.

4. Response properties for a cyclic shaking procedure

In this section we consider a shaking procedure defined as a sequence of steps where x is varied following a cycle or a more general function. A generic procedure is defined giving an initial and a final value of x, x_I and x_F, the maximal value of x, x_{max}, the value of the increments in x (in our simulations we have always used $\Delta x = 0.01$) and the time interval $\Delta\tau$ the system spends at each value of x. We have considered values of $\Delta\tau$ equal to 10^2, 10^3, 10^4 and 10^5. The two main procedures we have considered are defined in the following way:

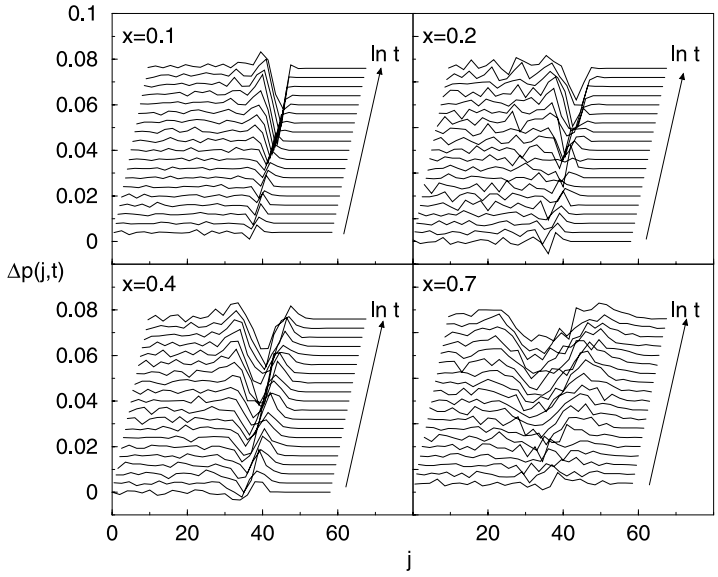

Figure 15. Temporal evolution ($t = 0$–10^6) of the difference between the density profiles of the perturbed and unperturbed systems, $\Delta p(j, t + t_w)$, after $t_w = 10^4$ and various values of x. Comparing this figure with figure 12, one observes that the dips and bumps are located near the interface, and they are larger for larger x, i.e. for a broader interface.

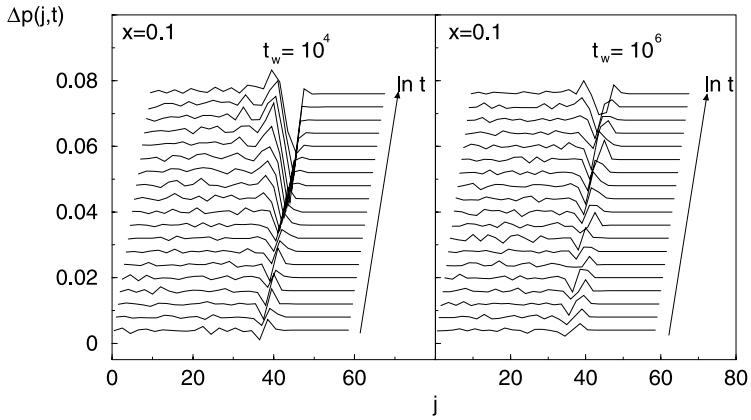

Figure 16. Temporal evolution ($t = t_w$ to $t = t_w + 10^6$) of the difference between the density profiles of the perturbed and unperturbed systems, $\Delta p(j, t + t_w)$, for $x = 0.1$ and two waiting times: $t_w = 10^4$ and 10^6. The larger t_w is, the slower the overall processes.

- *cycle*: an increase from $x_I = 0.01$ to $x_{max} = 0.8$, and then decrease to x_F;
- *cooling*: a simple decrease from $x_I = x_{max}$ ($x_I = 0.6,\ 0.7,\ 0.8,\ 0.9$) to x_F.

The final values of x were $x_F = 0.4,\ 0.2,\ 0.1$. Once the final value x_F of x was reached, x was kept constant and the measurements of the response function (with a copy evolving at $x + \mathrm{d}x$), the correlation function and the density profiles were done either without any further delay, or with an additional waiting time at constant $x = x_F$ of 10^4 or 10^5 time steps.

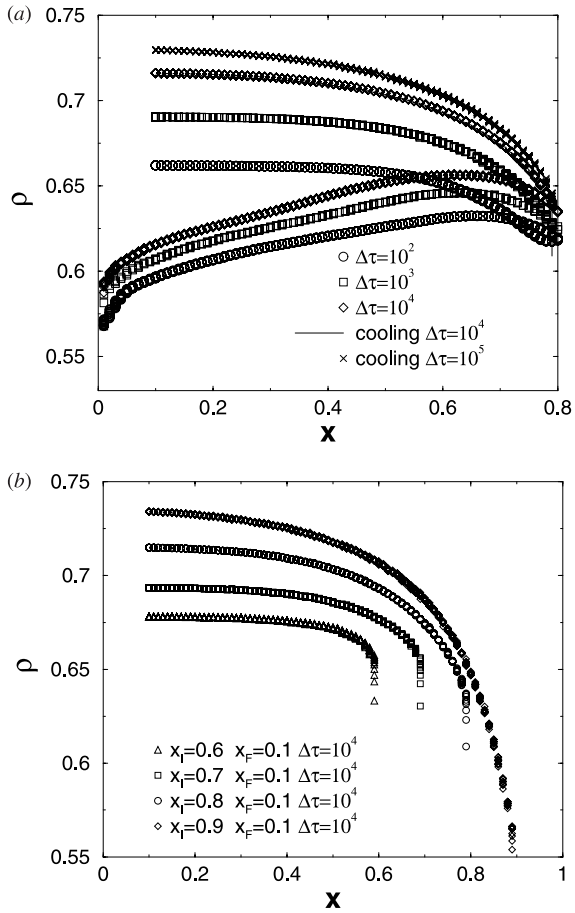

Figure 17. Bulk density versus x during the cycle (a) or cooling (b) procedures, for various values of $\Delta\tau$ and x_{max}. On (a) for comparison we show the behaviour of two cooling procedures with $\Delta\tau = 10^4$ and 10^5. We see that a simple cooling from x_{max} is equivalent to a cycle with the same x_{max}. In general, higher densities are obtained with slower procedures (larger $\Delta\tau$) or higher values of $x_{max} = x_I$.

We shall see that such procedures, similar to a slow cooling for thermal systems, allow one to reach large densities, seemingly unreachable at constant x. We note that these procedures are indeed those used experimentally to efficiently compactify granular systems. The examination of the density profiles will allow one to gain a deeper insight for the effectiveness of such cycles.

We first plot in figure 17 the evolution of the density during a cycle; the influence of $\Delta\tau$ is clear, and similar to the case of cooling: larger $\Delta\tau$ allows one to reach higher densities. Moreover, the obtained densities are impressively higher than the densities obtained at constant shaking amplitude.

We also checked that the part of the cycle with growing x has no practical use or influence on the 'cooling' part (see figure 17). Only the maximal value of x is relevant. This seems reasonable, since structures formed at low x are destroyed by a shaking at larger x. On the other hand, if $\Delta\tau$ is not very large, we have observed that a second cycle can be useful to obtain still higher densities. Figure 17(b) also shows that higher densities are obtained with higher values of x_{max}. This improving trend presents a saturation effect: given a certain value

of $\Delta\tau$, increasing x_{max} above 0.9 (we have checked this behaviour up to $x_{max} = 0.99$) does not allow one to increase the asymptotic density further. On the other hand, taking an x_{max} too small with a fixed $\Delta\tau$ or taking a $\Delta\tau$ too small brings the system out of the reversible branch. In this sense our results fit quite well with the experimental findings [10], where it is stated that there exists a Γ^* that defines an 'irreversibility point'. Only for $\Gamma_{max} > \Gamma^*$ is one always on the reversible branch. Moreover, a cooling from $\Gamma_{max} > \Gamma^*$ achieved with a too small $\Delta\tau$ brings the system out of equilibrium.

It is quite interesting to look at the density profiles at various x_F after a cycle (see figure 18). For $x_F = 0.1$, the bulk is much denser than after any reachable t_w at constant x, and the interface is as steep. (Note, however, that, for $\Delta\tau$ too small, there is still a dense layer at the interface for $x_F = 0.1$.) Moreover, at fixed x_I, a larger $\Delta\tau$ yields better compaction in the bulk, as does, at fixed $\Delta\tau$, a larger x_I.

The comparison of the profiles at $x_F = 0.4,\ 0.2$ and 0.1 (at fixed x_I and $\Delta\tau$) shows that the bulk parts of the profiles are identical: only the interfaces change and they are steeper for lower x. When x is lowered, the bulk retains its properties while the interface is gradually sharpened. This means that, in order to better compactify, one has to take into account that high values of x are effective for the bulk, while low values of x make the interface denser and steeper. Besides, the larger x_I (see figures 18(c) and (d)), the deeper the bulk is affected at the beginning of the cooling, the more compact the system is at the end of the cooling.

From these observations we deduce that the optimal method to compactify is to begin with a high x_I (but a too high value of x_I is not useful, since, as previously mentioned, its influence saturates), and decrease x as slowly as possible. If x_I is higher, then one is allowed to take a lower value of $\Delta\tau$, thus gaining time in the compaction process. Note moreover that, for $x_I = 0.9$, the difference between the profiles obtained at $\Delta\tau = 10^4$ or 10^5 is very small. Moreover, if only the bulk has to be compactified, one can stop the process at intermediate values of x (see figure 18) while, in order to also have a sharp interface, the process has to be continued down to low values of x. It would be interesting to carry out detailed experimental tests of these predictions.

After a cycle or a cooling procedure, the mass–mass two-times correlation function (figure 19) consistently shows an effective age of the system which is much larger than the real one: for example, for a global real time of 7×10^5 (cooling from $x_I = 0.8$ to 0.1 in steps of $\Delta x = 0.01$ with $\Delta\tau = 10^4$), the effective age is much larger than 10^6 (largest waiting time simulated at constant x). This fact is confirmed if we wait an additional $t_w = 10^4$ or 10^5 after the cycle: we observe time-translation invariance, showing that the system is in an equilibrium or quasi-equilibrium state.

The response function, shown in figure 20, is also independent of t_w (for $t_w = 0,\ 10^4,\ 10^5$), and is always positive.

Once again, this behaviour can be understood by the analysis of the difference of the density profiles of the two replicas. Figure 21 shows $\Delta p(j, t)$ for several combinations of x_I and x_F. This figure is to be compared with figure 15. In all cases one observes that the change in x_F only modifies the interface, broadening it. The interface in this case is always composed of a denser layer (bump) lying above a looser layer (dip). The only effect of the perturbation is a broadening of the interface, even at small x_F, thus causing a positive response, because the bulk has already been efficiently compactified by the cycling procedure.

5. Comparing different procedures: the importance of the history

In this section we try to give a unified picture of the results we have shown so far. Since in a granular system there is no dynamics without any energy injection, i.e. without any external

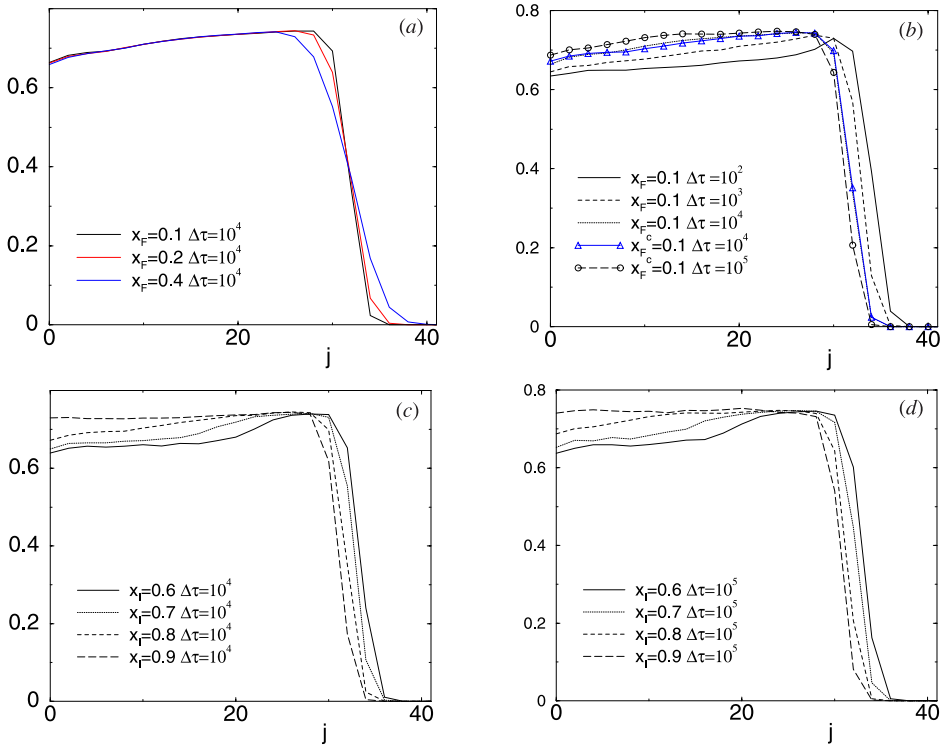

Figure 18. (*a*) Influence of x_F on the density profile after a cycle, for $x_{max} = 0.8$, $\Delta\tau = 10^4$; the bulk is not affected, but the interface is steeper for smaller x_F. (*b*) At constant $x_{max} = 0.8$ and $x_F = 0.1$, effect of $\Delta\tau$; the bulk is denser for larger $\Delta\tau$, while the steepness of the interface is not changed; $x_F = 0.1$ corresponds to a complete cycle, while $x_F^c = 0.1$ corresponds to a cooling from $x_{max} = 0.8$. We see that the two procedures are equivalent. (*c*) influence of $x_I = x_{max}$, at constant $\Delta\tau = 10^4$; the bulk is denser for higher x_I, the steepness of the interface is not changed. (*d*) The same for $\Delta\tau = 10^5$.

perturbations, it is highly important to deeply understand the response properties to such perturbations. One of the most important points to stress is the fact that the response is never homogeneous. One can never assume that the properties of the system are homogeneously distributed, not even assuming a coarse-grained point of view. The perturbations drive the system into an instability mechanism that generates large-scale spatial structures [7, 8]. Let us discuss the consequences of this phenomenon that has been called *self-organized structuring* [7].

First of all, one is not allowed to describe a static packing in terms only of a scalar quantity such as the density. It is evident how it is possible to construct several different packings corresponding to the same global average density, each one with completely different rheological properties (for a concrete example concerning the behaviour of a granular system subject to shearing see [5]). Recent experiments [17] have made this point clear. Depending on the properties investigated one is then forced to enlarge the parameter space in order to give a reasonable description of the system. One important ingredient to take into account is the history, e.g. the ensemble of dynamical procedures the system has undergone until the moment when we analyse it. One can then ask where the information about the past history is encoded and whether it is possible to take into account this history in some suitable coarsed-

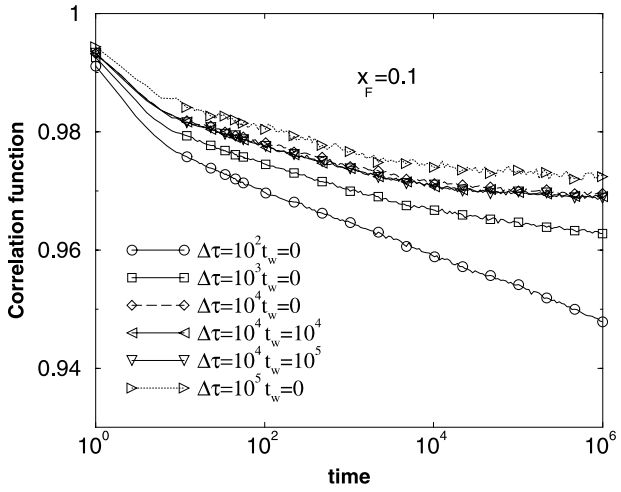

Figure 19. Correlation function after a cycle with $x_F = 0.1$, $x_{max} = 0.8$. The longer the cycle, the older the system looks (i.e. the slower the correlation decays). The curves for $\Delta\tau = 10^4$ with $t_w = 0,\ 10^4,\ 10^5$ are perfectly collapsed, showing time-translation invariance.

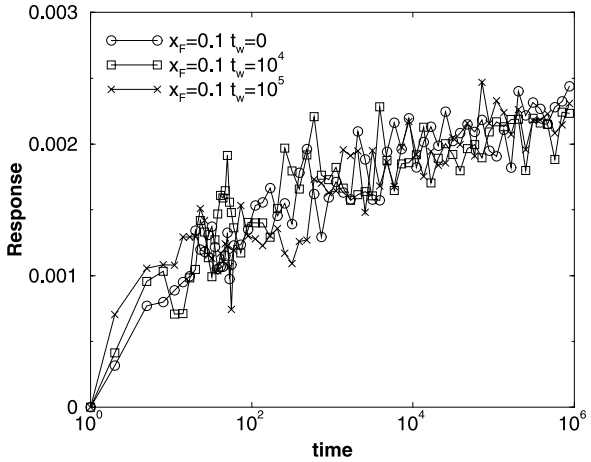

Figure 20. Response function after a cycle with $x_F = 0.1$ and 0.8, $x_{max} = 0.8$, and a time $t_w = 0,\ 10^4,\ 10^5$ at constant $x = x_F = 0.1$. The response is small with large fluctuations, but definitely positive. We show only the case $x_F = 0.1$, the response being an increasing function of x_F.

grained view. One possibility is to consider the density as a local parameter and describe the system in terms of some density map. It is precisely in this spirit that in this paper we have considered, as a first step in this direction, the analysis of the time evolution of the density profiles†. This corresponds to investigating the properties of the system in the direction of the imposed external field: the gravity.

The presence of large-scale structures in the system makes the problem of the response properties far from being trivial. One of the first questions one could ask concerns the best

† A further step in this direction is to consider the real two-dimensional density maps. For this we refer the reader to [2, 8].

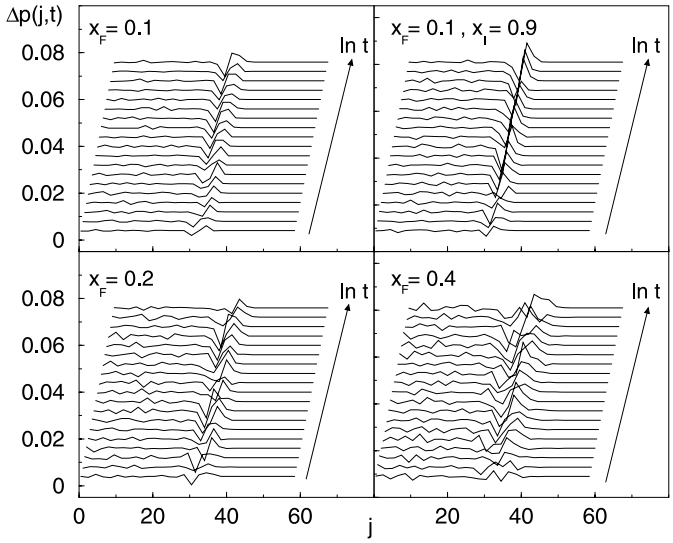

Figure 21. Temporal evolution (from $t = 0$ to 10^6) of the difference between the density profiles of the perturbed and unperturbed systems, $\Delta p(j, t)$, after a cooling from $x_I = 0.8$ to 0.1, 0.2, 0.4, with $\Delta\tau = 10^4$ (top left, bottom left and bottom right, respectively) or from $x_I = 0.9$ to $x_F = 0.1$ (with $\Delta\tau = 10^4$) (top right).

procedure to compactify a given sample. The best strategy refers to the strategy that allows one to obtain the highest density in a given time. Alternatively, one could consider the best strategy to reach a given density in the shortest time. Since different parts of the sample (in the zeroth-order schematization one can consider the bulk and the surface) respond in a different way to different values of the shaking amplitude x, it is obvious to conclude that the best strategy will not coincide with a procedure in which one keeps x fixed indefinitely. In this case, in fact, as we have shown in section 3, the average bulk density at a fixed time is not a monotonic function of x. It is then quite intuitive to figure out different procedures where x is a complex function of time. We have shown in section 4 that one of the best procedures is to consider a cooling process where one starts with a relatively high value of $x = x_{max}$ and progressively decrease x with a rate $1/\Delta\tau$ up to a final value x_F. The higher either x_{max} or $\Delta\tau$ are, the larger will be the final asymptotic density. The smaller the value of x_F, the larger the compactified region will be and the sharper the interface.

The rationale behind this definition of the optimal compaction procedure can be understood as follows. The best way to compactify the system globally is to start from the compaction of the bottom part of the system. In order to do this one should choose high values of x which allow one to extend the interface of the system, i.e. the mobilized region, deeper and deeper. The procedure then proceeds reducing the value of x progressively in order to compactify sequentially regions at larger heights. It is clear that a small value of x cannot affect the part of the system already compactified with a larger value of x. That is why in order to also better compactify the system interface one has to continue the procedure to very small values of x. In this way one can associate with each particular value of x during the procedure the optimal compaction of a specific region of the system. On the other hand, it is clear why the compaction process gives better results for larger $\Delta\tau$. Spending longer on a certain value of x allows one to better compactify the region corresponding to this value of x. The shaking procedure at constant x thus cannot be effective because a large x will only be able to compactify the deep

bulk while a small x will create a high-density layer below the interface (see figure 12) which for a very long time will stop the bulk compaction.

The presence of large-scale structures also causes many consequences in the behaviour of the response function as defined in equation (2). From the results presented in the previous sections, it is evident as, even in a very simplified picture, the sign of the response function depends on a complex convolution of several contributions: the spatial structures spontaneously emerging in the system (again at the zeroth order of approximation one can consider the sum of two coupled contributions coming from the surface and the bulk), the value of the shaking amplitude and the past history of the system (encoded in the value of t_w for a constant shaking amplitude or, more generally, in the whole definition of the dynamical procedure). It is then evident how trying to explain the results about the sign of the response function on only the basis of the shaking amplitude (x) can be fallacious. There does not exist, as suggested in [9], a transition in x such that the response function is positive above a certain value of x and negative below this value. In the case of constant shaking amplitude, no matter what the value of x is, one typically observes a positive response due to the contribution of the system surface, eventually followed by a negative regime at times that depend on x and t_w: the larger are x or t_w, the larger is the time over which one sees a positive response. This is due to the complex balance between the contributions coming from the surface and those from the bulk. These features were not considered in [9] where the role of inhomogeneities was neglected and where only small values of t_w were considered. On the other hand, if one looks at the response after a cyclic procedure, as described in section 4, one realizes that the response is always positive because in this case only the interface is giving an important contribution.

It is interesting to compare the results obtained for the mass–mass two-times correlation function using different driving procedures. We have shown in section 3 the presence of ageing in a system driven with a given constant x. In this case one observes a two-steps relaxation of the correlation function, typically observed in glassy systems. The second relaxation is quite well described by a function decaying as $\log(t_w)/\log(t + t_w)$ no matter the value of x. Similar behaviour has been observed for the mean-square distance between the potential energies, $B(t + t_w, t_w)$. On the other hand, the behaviour of the correlation function turns out to be completely different if the system is subject to a more complicated driving procedure. In section 4 we have shown that the use of a cyclic or of a cooling procedure brings the system into a state where time-translation invariance holds, i.e. there is no more ageing. Experiments analysing the presence or absence of ageing in granular material would certainly be welcome, and a first step is being taken in [17]. In this case the state reached by the system is such that the bulk is almost completely decoupled from the system interface, i.e. the bulk density no longer changes with time. At this stage the dynamics of the system is concentrated on the interface which is almost in an equilibrium state compatible with the final value of x, x_F. The system no longer ages and the global response (see figure 20) is always positive. For another approach to the relaxation dynamics of granular media that focuses on the asymptotic stationary state reached after a very long shaking procedure we refer the reader to [18].

These last observations raise a further question concerning the possibility of associating to a granular system a unique scalar temperature when the space translation invariance is broken. In [18] it has been shown that this is indeed possible if the system is in a stationary state. In this case one can show that it there exists a 'temperature'-like quantity which is made uniform everywhere in the system and which is related do the derivative of a suitable free-energy-like functional. It is evident how one immediately gets into trouble if the system is far from being homogeneous and if the presence of spatial structures is accompanied by a breakdown of the time-translation invariance (ageing behaviour). The above discussion about the sign of the response function represents an example of how data analysis can be misleading. It is

then clear how in general one cannot describe the response properties of a granular system in terms of a unique parameter, e.g. the temperature. Considering different values of x or t_w or considering different dynamical procedures, one is simply exploring different non-equilibrium regions of the phase space that correspond to different spatial inhomogeneities. From the above discussion it should be clear that a negative value of the response function does not mean that one can associate a negative effective temperature to the whole system [9] (in the spirit of the fluctuation–dissipation theorem (FDT) [19]). In this case one simply has that for the specific values of x and t_w explored, the contribution coming from the bulk is important. This contribution can change depending on the global history (which is encoded in the spatial structures), on x and t_w and thus, unless one is able to introduce more subtle, and local, indicators, it seems to us quite meaningless and misleading to try to extend to this case the definition of an effective temperature. From this point of view, unless one is able to define suitable free-energy-like functionals† taking into account the heterogeneities of the system, any statement about the validity of the fluctuation–dissipation theorem in such heterogeneous systems [9], which anyway has to be considered in the limit $t_w \to \infty$, seems to us hazardous.

We make a last remark concerning the effect of the boundary conditions on the results presented so far. Most of our results have been obtained with periodic boundary conditions and in this case we have checked how globally the results are qualitatively the same by changing the aspect ratio of the container. In particular, we have considered a wide range of situations from very tall containers such as those considered in the experiments [10] ($M = 200$, $L = 20, 40, 60$) to very wide systems ($L = 200$, $M = 60$). In order to mimic the effect of the real container walls we have also considered some cases with closed boundary conditions. In this case the walls are rigid and one does not allow overlaps between the particles and the walls. Also in this case we did not find any substantial difference in the main features of the model. The structure formation proceeds along the same lines as above and the only remarkable difference is a further slowing down of the process with respect to the periodic boundary conditions case.

6. Conclusions

In this paper we have investigated the response properties of granular media within the framework of a recently proposed class of models, the so-called random Tetris model. On the one hand, we focused our attention on global quantities such as the global density, the response and the correlation functions. On the other hand, we have monitored some local quantities that allowed us to investigate the large-scale structures spontaneously emerging in these systems as a response to the imposed perturbation (driving). The comparison between global and local quantities allowed us to gain a deeper insight into how granular materials respond to perturbations and in this perspective of the importance of spatial structures. We have considered several different perturbation procedures defined in terms of the temporal functions describing the shaking amplitude (Γ in the experiments and x with $\Gamma \simeq 1/\log(1/\sqrt{x})$ in the models). In particular, we have analysed the case where one keeps x indefinitely constant and compared this case with that where x varies as a function of time, $x(t)$. Our main results can be summarized as follows. In the case of a procedure at constant x the system exhibits ageing described by a correlation function decaying as $\log(t_w)/\log(t + t_w)$. The response function exhibits a complex behaviour depending on x and t_w. In general, one always observes a positive response eventually followed, at times increasing with either x or t_w, by a negative response. All these properties can be explained by looking at the heterogeneities arising in the density profiles.

† It is interesting in this perspective to look at [20].

The scenario changes completely when considering more complex shaking procedures where $x = x(t)$. In this case (see section 4 for the details) the system can be found in an almost stationary state where ageing is no longer present, i.e. the correlation function is time-translation invariant, and the response function is always positive. Also in this case the comparison of the results with the analysis of the density profiles allows us to gain a deeper understanding of the effect of the perturbation on the system. On this basis we are able to formulate some specific recipes for the best compaction procedure and to comment on some recent results concerning the validity of the fluctuation–dissipation theorem and the possibility of a thermodynamic description for these non-thermal systems.

Let us conclude with two points that open possibilities for future work.

(a) Recent experiments [17] have focused on the response, not to a slight change in the forcing, but rather to a large change, in the spirit of experiments of temperature cycling in spin-glasses [21]. Work is in progress to reproduce the preliminary experimental results and draw comparisons with the spin-glasses phenomenology.
(b) We have defined the response function, as in [9], as the response of the system to a change in the driving force, which is itself considered as an analogue of the temperature. In order to try to understand whether an extension of the FDT can be thought of, it would probably be more reasonable to look at the response to a force acting randomly on the particles, and in a way uncorrelated to the overall driving, in a way similar to that used in a lattice-gas model [22] or in models of super-cooled liquids [23].

Needless to say, finally, it would be extremely important to have an experimental check of our predictions to be used as a starting point for further theoretical investigations.

Acknowledgments

We thank C Josserand and P Viot for discussions and communication of results prior to publication. VL acknowledges financial support under project ERBFMBICT961220. This work has been partially supported from the European Network-Fractals under contract no FMRXCT980183.

References

[1] Herrmann H J *et al* (ed) 1998 *Proc. NATO Advanced Study Institute on Physics of Dry Granular Media* (Dordrecht: Kluwer)
[2] Caglioti E, Krishnamurthy S and Loreto V 1999 unpublished
[3] Caglioti E, Loreto V, Herrmann H J and Nicodemi M 1997 *Phys. Rev. Lett.* **79** 1575
[4] Caglioti E, Coniglio A, Herrmann H J, Loreto V and Nicodemi M 1998 *Europhys. Lett.* **43** 591
[5] Piccioni M, Loreto V and Roux S 2000 *Phys. Rev.* E **61** 2813
[6] Nicodemi M and Coniglio A 1999 *Phys. Rev. Lett.* **82** 916
[7] Krishnamurthy S, Herrmann H J, Loreto V, Nicodemi M and Roux S 1999 *Fractals* **7** 51–8
Krishnamurthy S, Loreto V, Herrmann H J, Manna S S and Roux S 1999 *Phys. Rev. Lett.* **83** 304
Krishnamurthy S, Loreto V and Roux S 2000 *Phys. Rev. Lett.* **84** 1039
[8] Baldassarri A, Krishnamurthy S and Loreto V 2000 unpublished
[9] Nicodemi M 1999 *Phys. Rev. Lett.* **82** 3734
[10] Knight J B, Fandrich C G, Lau C N, Jaeger H M and Nagel S R 1995 *Phys. Rev.* E **51** 3957
Nowak E R, Knight J B, Povinelli M, Jaeger H M and Nagel S R 1997 *Powder Technol.* **94** 79–83
Nowak E R, Knight J B, Ben-Naim E, Jaeger H M and Nagel S R 1998 *Phys. Rev.* E **57** 1971–82
Jaeger H M 1998 *Physics of Dry Granular Media* ed H J Herrmann, J P Hovi and S Luding (Dordrecht: Kluwer) pp 553–83
[11] Talbot J, Tarjus G and Viot P 2000 *Phys. Rev.* E **61** 5429
(Talbot J, Tarjus G and Viot P 1999 *Preprint* cond-mat/9910239)

[12] Duran J, Mazozi T, Clément E and Rajchenbach J 1994 *Phys. Rev.* E **50** 3092
[13] See, for instance, Boutreux T and de Gennes P G *Powders and Grains '97* ed R Behringer and J Jenkins (Rotterdam: Balkema) p 439
Ben-Naim E, Knight J B and Nowak E R 1998 *Physica* D **123** 380
Krapivsky P L and Ben-Naim E 1994 *J. Chem. Phys.* **100** 6778
Nicodemi M, Coniglio A and Herrmann H J 1997 *Phys. Rev.* E **55** 1
[14] See, for example, Bouchaud J P, Cugliandolo L F, Kurchan J and Mézard M 1997 *Spin Glasses and Random Field* ed A P Young (Singapore: World Scientific)
[15] Bouchaud J P 1995 *J. Physique* I **2** 265
[16] Viot P 1999 Private commununication
[17] Josserand C, Tkachenko A, Mueth D M and Jaeger H M 2000 Memory effects in granular material *Phys. Rev. Lett.* at press (*Preprint* cond-mat/0002401)
[18] Caglioti E and Loreto V 1999 *Phys. Rev. Lett.* **83** 4333
[19] Cugliandolo L F, Kurchan J and Peliti L 1997 *Phys. Rev.* E **55** 3898
[20] Edwards S F 1990 *Current Trends in the Physics of Materials* (Amsterdam: North-Holland)
Edwards S F and Oakeshott R B S 1989 *Physica* A **157** 1080
Edwards S F and Mounfield C C 1994 *Physica* A **210** 279
Edwards S F and Grinev D V 1999 *Phys. Rev.* E **58** 4758
[21] See, e.g., Vincent E, Hammann J, Ocio M, Bouchaud J P and Cugliandolo L F 1997 *Spin Glasses and Random Field* ed A P Young (Singapore: World Scientific) and references therein
[22] Sellitto M 1998 *Eur. Phys. J.* B **4** 135
[23] See, e.g., Parisi G 1997 *Phys. Rev. Lett.* **79** 3660
Kob W and Barrat J L 2000 *Eur. Phys. J.* B **13** 319
Kob W and Barrat J L 1999 *Physica* A **263** 234